RESEARCH PAPER

Experimental study and comparison of the use of solar cells as desalination units in water production

Hassan S. Abdelamir*, Dhafer M. Hachim, Ali N. Al-Shamani

Engineering Technical College of Najaf, Al-Furat Al-Awsat Technical University, Najaf, Iraq

Abstract

Numerous researchers have examined alternative and safe techniques for desalinating water in arid regions. The most optimal and cost-effective approach is desalination through solar energy, owing to its widespread availability and lack of detrimental effects on the environment. Solar cells possess diverse applications, one of which is desalination. The present study presents a novel method for desalinating brackish water and seawater utilizing solar energy. The procedure involved the evaporation of water through the sun's radiation in a controlled setting. The experimentation was conducted within the confines of the laboratory at Najaf Engineering Technical College. The fresh design of the solar active photovoltaic distiller incorporates a solar photovoltaic Peltier system. The outcomes of the experiment demonstrated that incorporating three Peltiers within the glass and wick proved superior to their external placement, resulting in an augmented production of distilled water. The cumulative productivity achieved when employing three Peltiers inside the glass at flow rates of 1, 2, and 4 ml/min were 502, 967, and 1319 g, respectively. In contrast, the productivity amounted to 325, 627, and 1000 g when utilizing three Peltiers outside the glass at the same flow rates. The main objective of this study was to develop and assess a solar still with a solar cell, aiming to maximize productivity per unit area; the findings revealed that the third model, incorporating internal Peltiers, achieved higher overall productivity compared to the second model, primarily due to the Peltiers' capability to control temperature within the distiller, thereby enhancing condensation efficiency.

Keywords: Enhance productivity, Freshwater, Peltier, Solar cell, Solar water desalination, Wick

1. Introduction

The utilization of solar energy concentrators is a recommended solution for meeting global energy needs due to the potential to harness the thermal energy associated with reflected rays. Solar concentrators have various applications, including solar water desalination systems, solar heaters, and cookers. The effective management of existing freshwater resources is of utmost importance in order to increase the availability of freshwater. The demand for freshwater has risen consistently over the past two centuries as a result of population growth and industrialization. However, the supply of freshwater has remained constant and is now dangerously close to depletion. The primary source of freshwater is rainfall, which is generated through the hydrological cycle. However, the amount of rainfall varies significantly depending on geographical location due to various environmental factors. Consequently, providing freshwater to meet the growing demand becomes extremely challenging. Nevertheless, there are alternative methods for obtaining potable water beyond relying solely on the natural water cycle. Developing innovative techniques that effectively utilize the currently available resources is crucial to increasing the production of freshwater.[1–3]

In the pursuit of generating electricity and purifying water, photovoltaic (PV) panels are utilized. There have been cautious attempts to produce freshwater consistently. These panels are composed

Received 2 November 2023; revised 5 December 2023; accepted 10 July 2024.
Available online 19 September 2024

* Corresponding author at: Engineering Technical College of Najaf, Al-Furat Al-Awsat Technical University, Najaf 31001, Iraq.
E-mail address: hassan.ms.etcn11@student.atu.edu.iq (H.S. Abdelamir).

https://doi.org/10.62593/2090-2468.1042

of a glass casing and a solar-powered charging system. Kumar and Tiwari[4] in this paper estimate the internal heat transfer coefficients of a hybrid (PV/T) active solar still based on outdoor experimental observations. The average annual values of convective heat transfer coefficient for the passive and hybrid (PV/T) active solar still are observed as 0.78 and 2.41 W/m^2/K, respectively, at 0.05 m water depth. Dev and Centre[5] in this article introduce two analytical techniques for determining the characteristic equation of a hybrid active solar still, one involving the plotting of linear and nonlinear curves and the other employing a matrix method; the nonlinear equation is found to outperform the linear equation, as evaluated by the root mean square percentage error.[6] They present a self-sustainable hybrid PV/thermal (PV/T) active solar still suitable for remote areas with ample solar energy. Experimental results demonstrate significantly higher daily yield, 32 and 55 times greater in summer and winter, respectively, compared to passive solar still, with higher electrical and thermal efficiency. Gaur and Tiwari[7] work to enhance the efficiency of a PV/T hybrid active solar still by integrating the collectors with the basin. The research demonstrates that the optimum number of collectors is influenced by the water mass in the basin, with the highest yield observed at $N = 4$ for 50 kg of water mass based on exergy efficiency, and the thermal model has been validated experimentally. Eltawil and Omara[8] improve the efficiency of a solar still for communities that lack electricity and clean water. The developed solar still showed a productivity increase of 51–148% compared to the conventional solar still, depending on the amendment used. The use of an external condenser increased productivity by 51%, while the use of circulated hot water in passive and active sprays without a condenser led to increases of 56 and 82%, respectively. Overall, the developed solar still demonstrated its suitability for desalination when suitable weather conditions and moderate water demand are present. Saeedi et al.[9] they are focused on optimizing a PV/T active solar still by deriving analytical expressions for temperatures and water productivity, calculating electrical power using an I–V model, comparing simulation results with experimental data, and determining optimized values for mass flow rate, number of collectors, and objective function while also investigating the impact of operating parameters on energy efficiency. Al-Nimr and Al-Ammari[10] present a new PV/T-distillation system comprising a single slope basin solar still with a PV/T cell at the bottom and an external finned condenser and a mathematical model is developed to analyze its performance, which shows agreement with previous studies, and the impact of solar radiation, wind speed, ambient temperature, and the condensing chamber is also examined. Tiwari et al.[11] in this paper primarily focus on the analysis and evaluation of the proposed PVT-FPC active solar distillation system and provide equations for cost calculations. While Yari et al.[12] propose and analyze a new solar still equipped with semitransparent PV and evacuated tube collector in natural mode. Also Riahia et al.[13] evaluated the performance of a double slope solar still integrated with a 500 W heater powered by six PV modules connected to four batteries to produce potable water. As well as Pansal et al.[14] integration of active solar still with PV panel to increase distillate output and improve efficiency of solar PV. While Abed et al.[15] on a hybrid PV/T system for distillate water production. Utilizes passive cooling technique to obtain freshwater from PV panels. Investigates performance in terms of distilled water yield and power production. Different mass flow rates in the inner and outer wicks affect water production.

In this study, a novel concept of utilizing a solar distillation apparatus is presented, which aims to optimize space utilization and enhance the efficiency of solar energy conversion. The study investigates the integration of wick materials as used by Abed et al.[15] and added Peltier with PV systems, with a focus on inducing evaporation and condensation of water during the winter season. Experimental data collected indoors during winter showed promising results in terms of productivity and spatial coverage, which were then compared to previous research findings.

2. Experimental methods

Three models that make up the suggested design are as follows:

2.1. Model 1 (only photovoltaic)

An innovative solar energy capture model is developed in this research, as shown in Fig. 1. In accordance with the properties of the PV panel that

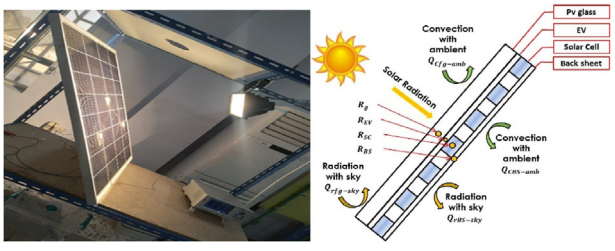

Fig. 1. Front view and scheme of Model 1.

was utilized, as stated in Table 1, the area was 0.6 m^2, and the inclination angle of the PV cell and solar panel was set to 54°. The PV panels served as the basis for the suggested new concept. In our experimental work, we want to decrease surface area and boost productivity simultaneously.

2.2. Model 2 (photovoltaic with wick and three Peltier's inside glass cover)

Model 2 is similar to Model 1, but with additional components such as a wick, an aluminum layer, an air gap, and a glass cover. Plain flat cotton and screen aluminum are used on the back face of the PV panel. The aluminum used in both screens and wicks has specific characteristics. To accommodate a PVC pipe, a hole is drilled into one side of the PV frame's side edge. Valves are spaced along the plastic tube, and a plastic tank with a linked hose is used. A manual primary valve controls the water flow, and a graduated cylinder is used to manage the water flow speed. A manual secondary valve is installed at the end of the cylinder. A baffle is installed on the back face of one PV panel to drain extra water. A cotton wick is inserted into an excavation, and the water is collected using a plastic pipe. Condensation occurs on the glass cover. Gaps and holes between the back glass cover are filled with silicone adhesive tape. The Peltier thermoelectric device transfers heat from one side to the other when a direct current is applied. P-type and n-type semiconductors are used in the device. The Peltier device used in the model is TEC1-12706, which has a Peltier element and a fan/heat sink system. Peltier materials consist of thermocouples sandwiched between ceramic plates, as shown in Fig. 2.

2.3. Model 3 (photovoltaic with wick and three Peltier's outside glass cover)

It is the same as Model 2, with the addition of a Peltier from outside the synthetic glass cover, as shown in Fig. 3.

Table 1. Properties photovoltaic.

Hengl solar	Photovoltaic module HL36P100
Rated power (−0; +5 W) (Pmpp)	100 W
Open circut voltage (Voc)	21.5 V
Short circut current (ISC)	6.28 A
Voltage at Pmpp (Vmpp)	17.5 V
Current at Pmpp (Impp)	5.71 A
Max. system voltage	1000 V
Cell efficiency	20.66%
Length and width	92 × 67 cm

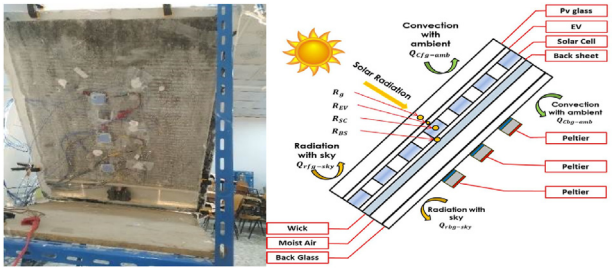

Fig. 2. Back view and scheme of Model 2.

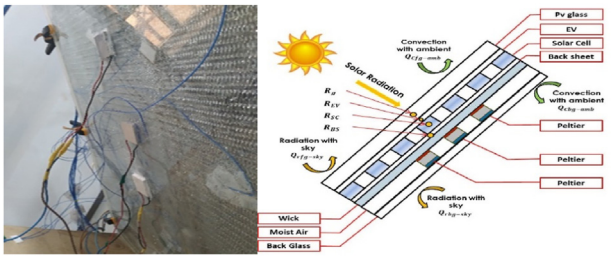

Fig. 3. Back view and scheme of Model 3.

3. Measurement device

Temperature measurements in a temperature measurement system were conducted using type K thermocouples. A total of 24 thermocouples were utilized with a precision of 0.2% ± 1 °C. The measurements included three thermocouples for the PV glass surface, five for the PV sheet back, four on a cotton wick, four aluminum rods for inside and outside the PV glass, and three for industrial glass and ambient temperature. All thermocouples were securely fastened using silicone and adhesives.

The solar power meter employed in this study measures the solar radiation received by PV panels. It features a calibration button that can set the instrument reading to 0 W/m^2 in complete darkness. The experiment ensured consistent solar radiation intensity over time by utilizing steady halogen light. Multiple readings of sun radiation intensity were taken at various heights between the industrial radiation source and the PV panel. The solar power meter is equipped with an LCD screen and sensor, as depicted in Fig. 4.

The solar module analyzer, displayed in Fig. 4, is a valuable tool for assessing PV panel parameters. It can generate curves, determine maximum solar energy, and calculate maximum voltage and current. The analyzer's software, coupled with a USB optical cable, enables the storage and analysis of test data on computers.

4. Uncertainty analysis

The external uncertainty is mostly caused by the measurement tools used during the experiment.

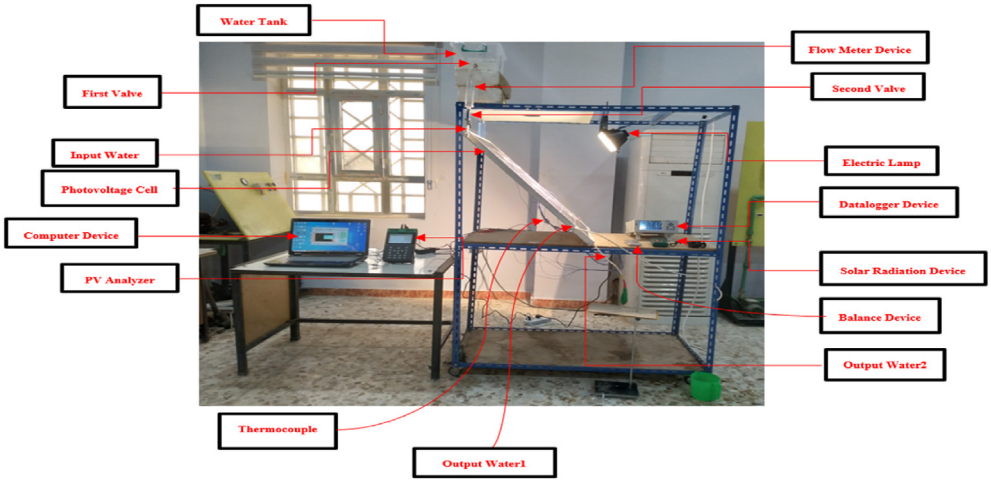

Fig. 4. The experimental rig and measurement device.

The precision of the measurements may be impacted by this instrument uncertainty. Several tools are used to monitor various factors, including the solar power meter, anemometer, measuring beaker, and solar module analyzer. This situation's normal level of uncertainty can be expressed as:

$$U = \frac{a}{\sqrt{3}} \tag{1}$$

Where a and U stand for, respectively, the standard uncertainty and the accuracy of the measuring tool. Table 2 provides a summary of the standard uncertainty, accuracy range, and instrument values.

4.1. Energy balance

4.1.1. For PV only – model 1

Glass layer:

$$M_{fg}\, C_{fg}\, \frac{dT_{fg}}{dt} = R_g - Q_{rfg-sky} - Q_{Cfg-amb} - Q_{COfg-EV} \tag{2}$$

Where all parameters of equation (2) are explained by Abed et al.[15]

EV layer:

$$M_{EV}\, C_{EV}\, \frac{dT_{EV}}{dt} = R_{EV} - Q_{COEV-SC} - Q_{COEV-fg} \tag{3}$$

Where all parameters of equation (3) are explained by Abed et al.[15]

Solar cells:

$$M_{SC}\, C_{SC}\, \frac{dT_{SC}}{dt} = R_{SC} - Q_{COSC-EV} - Q_{COSC-t} - Q_{ele} \tag{4}$$

Where all parameters of equation (4) are explained by Abed et al.[15]

Back sheet (Tedler layer):

$$M_{BS}\, C_{BS}\, \frac{dT_{BS}}{dt} = R_{BS} + Q_{COBS-SC} - Q_{CBS-amb} - Q_{rBS-sky} \tag{5}$$

Where all parameters of equation (5) are explained by Abed et al.[15]

4.1.2. For PV with wick and Peltier (outside)

Back sheet (Tedler layer):

$$M_{BS}\, C_{BS}\, \frac{dT_{BS}}{dt} = R_{BS} + Q_{COBS-SC} - Q_{CBS-wi} \tag{6}$$

Where all parameters of equation (6) are explained by Abed et al.[15]

Wick layer:

$$M_{wi}\, C_{w\,i}\, \frac{dT_{wi}}{dt} = Q_{CBS-wi} - Q_{rwi-bg} - Q_{ewi-ma} - Q_{cwi-ma} + c_w\, m_{in}\, T_{w,in} - c_w\, m_{ex}\, T_{w,ex} \tag{7}$$

Table 2. Uncertainty and accuracy of the measuring devices.

Tools	Ranges	Accuracy	Standard instruments uncertainty	Parameter measured
Solar module analyzer type PROVA 200 A	10–60 V	1 V	0.57	Voltage of the panel
	1–6 A	1 A	0.57	Current of the panel
Solar power meter type TENMARSTM-207	0–1999 W/m^2	10 W/m^2	5.6 W/m^2	Global radiation
Thermometer type (AT-4532x)	−50–1000 °C	1 °C	0.6 °C	Temperature

Where all parameters of equation (7) are explained by Abed et al.[15]

Moist air:

$$M_{ma}\,C_{ma}\frac{dT_{ma}}{dt}=Q_{ewi-ma}+Q_{Cwi-am}-Q_{Cma-bg}-Q_{Cdma-bg} \tag{8}$$

Where all parameters of equation (8) are explained by Abed et al.[15]

Back glass cover:

$$M_{bg}\,C_{bg}\frac{dT_{bg}}{dt}=Q_{cdma-bg}+Q_{Cma-bg}-Q_{Cbg-amb}-Q_{rbg-sky}-Qc \tag{9}$$

Where all parameters can be calculated by using equations (1)–(3) and (6) from Najafi and Woodbury.[16]

$$Q_c=S_m\,I_c\,T_c-\frac{I^2R_m}{2}-K_m\Delta T \tag{10}$$

The rejected heat from the hot side of the TEC module can be calculated[16]:

$$Q_h=S_m\,I_c\,T_h+\frac{I_c^2R_m}{2}-K_m\Delta T \tag{11}$$

4.1.3. For PV with wick and Peltier (inside)

The Model 3, similar to Model 2, employs three Peltier devices. However, the discrepancy between these two models lies in the placement of the Peltier device. In Model 3, the Peltier device is situated internally, whereas in Model 2, it is located externally, as depicted in Figs. 2 and 3. Consequently, this alteration in location leads to modifications in the heat balance equations of both the wick layer and the back glass layer, as follows:

Wick layer:

$$M_{wi}\,C_{w\,i}\frac{dT_{wi}}{dt}=Q_{CBS-wi}-Q_{rwi-bg}-Q_{ewi-ma}-Q_{cwi-ma}+c_w\,m_{in}\,T_{w,in}-c_w\,m_{ex}\,T_{w,ex}+Q_h \tag{12}$$

Back glass cover:

$$M_{bg}\,C_{bg}\frac{dT_{bg}}{dt}=Q_{cdma-bg}+Q_{Cma-bg}-Q_{Cbg-amb}-Q_{rbg-sky}-Qc \tag{13}$$

5. Result and discussion

5.1. Model 1 (PV only)

The task was performed for four straight hours within the room using one of the PV panels, which was angled at 54°. Solar radiation is steady at 637 W/m^2. Fig. 5a illustrates how the average PV glass temperature and PV back sheet temperature change over time. Keep in mind that after an hour, the temperature reaches the study state, where the average temperature for the front PV, back PV, and ambient temperature after 1 h is roughly (64.12, 56.83, and 22.29 °C). Additionally, keep in mind that the heat produced by solar radiation (IR) conversion to heat causes the temperature of PV to rise, which lowers PV efficiency. The relationship between power and voltage over time is depicted in Fig. 5b. Because of the falling current, power and voltage have increased.

5.2. Models 2 and 3

Figs. 6–8 provide a visual representation of the comparison made among the three selected models in the laboratory setting. The purpose of Fig. 6 is to showcase the temporal variation of the glass temperature of the solar cell. The findings obtained from this figure clearly demonstrate that during the initial 30-min period of the experiment, the temperature of

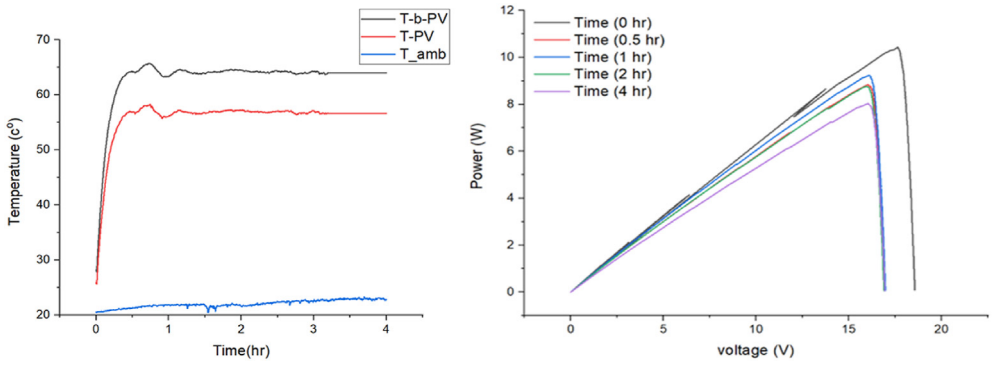

Fig. 5. (a) Temperature of only PV, (b) relation between power and voltage of PV.

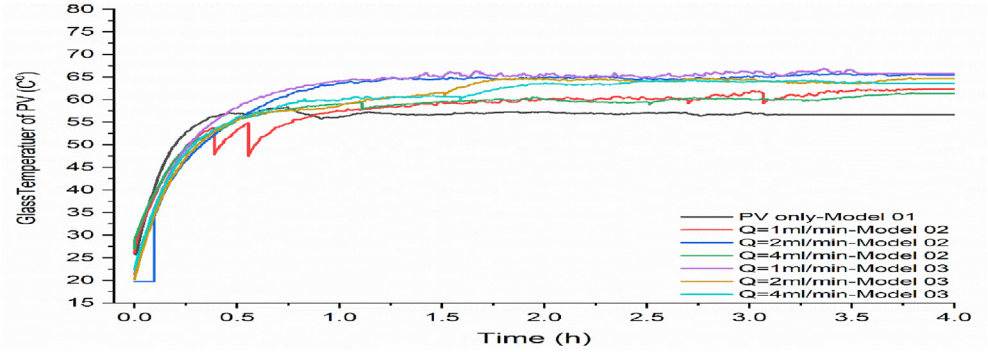

Fig. 6. Glass temperature of PV for three models with different water flow rates.

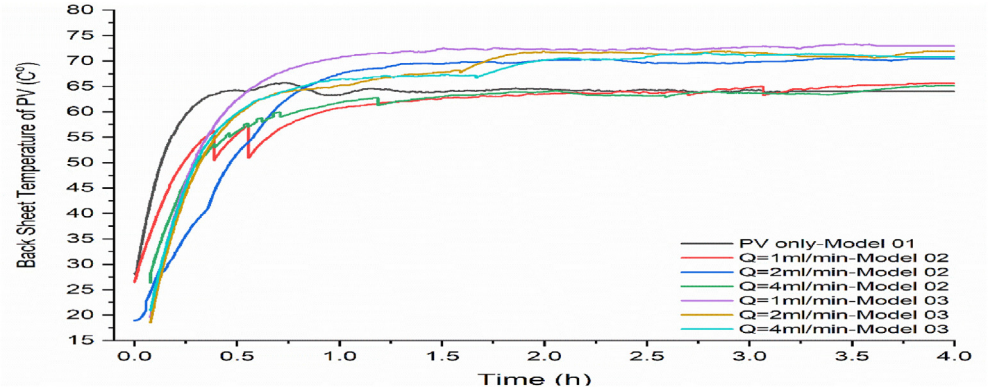

Fig. 7. Back sheet temperature of PV for three models with different water flow rates.

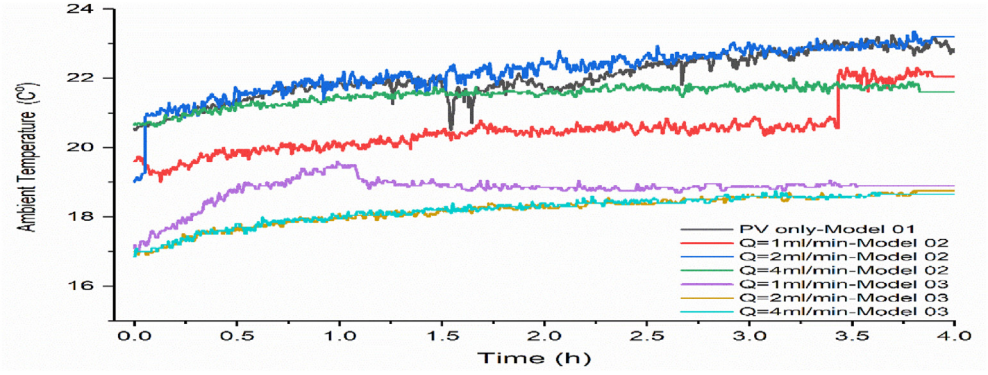

Fig. 8. Ambient temperature of three models with different water flow rates.

the glass was lower in the second and third models in comparison to the first model. However, as time progressed, an interesting shift occurred whereby the temperature of the first model became lower than that of the second and third models. The fluctuation in temperature can be attributed to the rapid evaporation process of the water in the wick positioned behind the cell at the start of the experiment. Consequently, this evaporation process effectively cools down the cell. However, after the initial 30-min mark, the evaporation process escalates, increasing in steam volume. This increase in steam volume then has an adverse effect on the performance of the cell. The occurrence of global warming in the condensation area situated behind the cell is the main cause of this adverse effect. The information depicted in Fig. 7, which showcases the temporal change in temperature behind the cell for all models, reveals that the second and third models consistently exhibited lower temperatures for the initial hour compared to the first model. Additionally, the results also indicate that the second model, at a water flow rate of 1 and 4 ml/min, closely approximated the temperature of the first model. This can be attributed

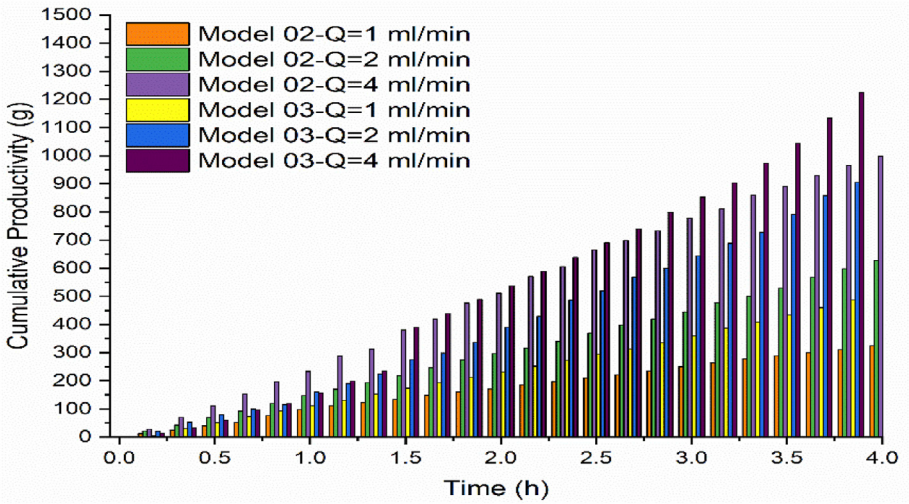

Fig. 9. Cumulative productivity of Model 2 and Model 3.

to the fact that the ambient temperature during the testing phase was lower than that of the first model. This relationship between the ambient temperature and the time is illustrated in Fig. 8, which provides valuable insights into the variation of the ambient temperature over time for all models.

The primary objective of this investigation is to fabricate and evaluate a solar still that incorporates a solar cell, aiming to achieve the greatest productivity per unit area. Fig. 9 displays the cumulative productivity of the second model at various flow rates, resulting in cumulative productivity values of 325, 627, and 1000 g at flow rates of 1, 2, and 4 ml/min, respectively, utilizing three external Peltiers to enhance condensation efficiency. Additionally, also Fig. 9 illustrates the productivity of the third model, which employs three Peltiers internally, yielding cumulative productivity values of 502, 967, and 1319 g at flow rates of 1, 2, and 4 ml/min, respectively, with the third model exhibiting higher productivity due to the Peltiers' positioning to enhance both evaporation and condensation.

5.3. Conclusions

Many researchers regard solar distillation as a significant method for utilizing solar energy to address issues of water scarcity. The solar still, a straightforward apparatus, proves effective in the conversion of brine into potable water. In conclusion, it is evident that:

(1) The findings indicate that the temperature of the glass was initially lower in the second and third models, but later, the first model had a lower temperature. This fluctuation is due to the evaporation process of the water in the wick behind the cell.
(2) The primary objective of this study was to create and evaluate a solar still that incorporates a solar cell, with the aim of achieving maximum productivity per unit area. The results indicated that the third model, which utilized internal Peltiers, yielded higher cumulative productivity compared to the second model, primarily due to the Peltiers' ability to manipulate temperature within the distiller.
(3) Using the Peltiers enhanced condensation efficiency by absorbing heat and adjusting temperature levels in the evaporation and condensation areas.
(4) The productivity of Model 2, expressed in kilograms per unit area and hour, is recorded as 0.135, 0.261, and 0.416 kg/m^2 h for flow rates of 1, 2, and 4 ml/min, respectively.
(5) The productivity of Model 3, as measured in kilogram per unit area and hour, exhibits values of 0.209, 0.403, and 0.550 kg/m^2 h when subjected to flow rates of 1, 2, and 4 ml/min, respectively.
(6) One of the significant constraints of using a wick in the back of a PV system is that it may lose efficiency over time due to the accumulation of salts.
(7) The future work involves investigating the use of a new type of wick material to enhance the evaporation rate, while being resistant to cumulative salts.

Author contribution

Hassan S. Abdelamir: Data curation, Writing-Original draft preparation, Conceptualization, Methodology, Software, Investigation, Validation. Dhafer Manea Hachim: Conceptualization, Methodology,

Supervision, Software, Investigation, Validation. Ali N. Al-Shamani: Supervision.

Funding

The entire work of this article is funded by the authors and there is no governmental or community funder.

Conflict of interest

The authors declare that they have no known competing financial interests or personal relationships that could have appeared to influence the work reported in this paper.

Appendix.

Appendix A

Measurement instruments used and procedures

Measurement instruments. All experiments in this work were conducted at the College of Technical Engineering, Najaf/Iraq (54). These experiments were performed with the help the main devices. Each of these devices will be explained as follows. When the pure water flows from the solar distillation pool, it falls from the distillation channel and is collected in a balloon. Every 10 min distilled water is recorded inside the balloon with a scale after weighing the balloon while it is empty.

Thermometer: Type K thermocouples are used to take temperature readings at various locations in a temperature measurement system. The number of thermocouples was 24 to record the temperature. It was accurate (0.2%±1Co). In this work measure the temperature of glass surface of PV (Three thermocouples as show in figure A1-a), sheet back PV (Five thermocouples as show in figure A1-b), cotton wick and screen alumnus (Four of them are mounted on a cotton wick, as well as four aluminum rods of thermocouples as show in figure A1-c), inside and outed glass cover (Three thermocouples were used to cover the inner side of the industrial glass, as well as three thermocouples for the outside of the glass as show in figure A1-d.) and ambit (Two were installed at ambient temperature and placed in a well-ventilated area of the thermocouple inside the chamber). Silicone and adhesives were also used to hold the thermocouples well as show in figure (A1-e).

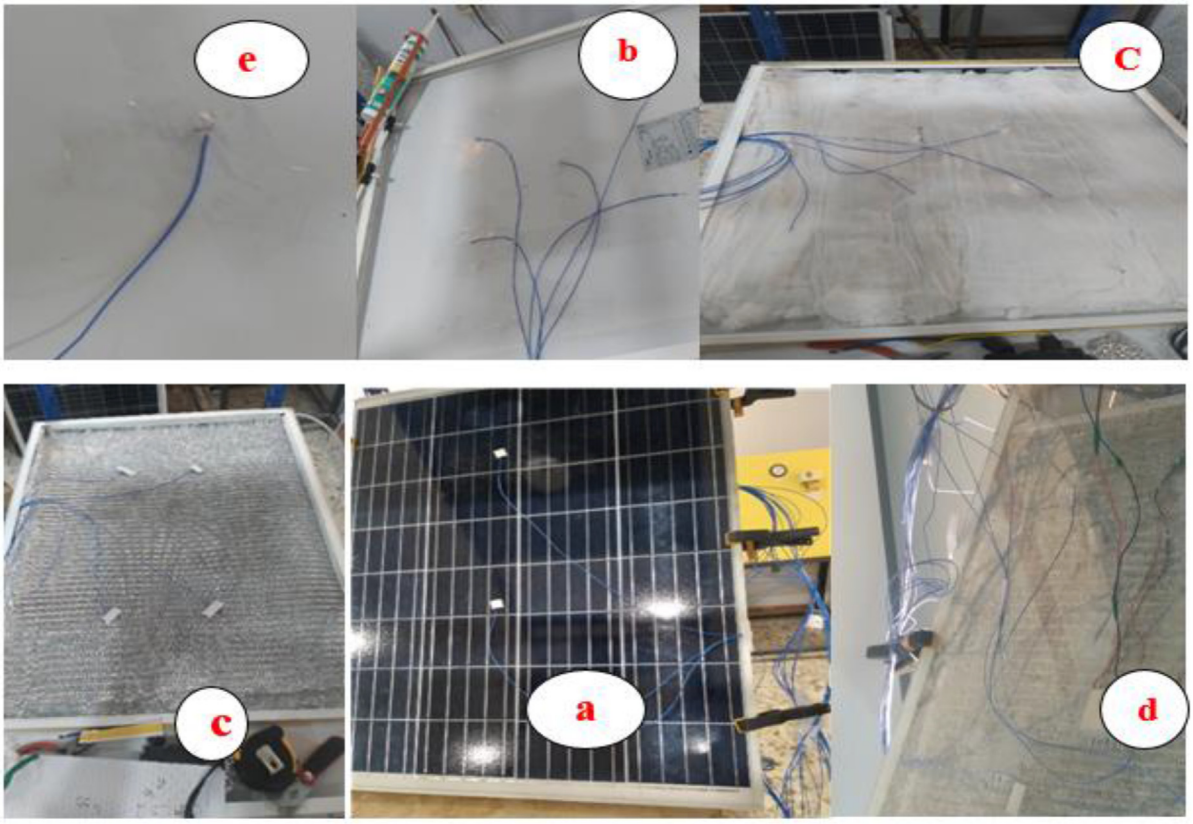

Fig. A1. Location of the thermocouples (a-glass surface of PV, b-sheet back PV, c-cotton wick and screen alumnus, d-inside and outed glass cover, e–Silicone and adhesives).

Solar Power Meter: The intensity of the solar radiation that is falling on the PV panels is measured using this solar power meter, the solar power meter has a calibration button that can be used to set the instrument's reading amount to (0) W/m2 while reading the device in complete darkness. Numerous readings of sun radiation intensity were taken at various heights between the source of industrial radiation and the PV panel because halogen light is stable at constant voltage and current, the intensity of solar radiation in this experiment is constant throughout time. Where the maximum radiation power reads about 2000 w/m^2 the solar power meter an Accuracy (±5%, ±10 W/m^2), As seen in Figure A2.

Fig. A2. Solar Radiation.

PV analyzer: The solar module analyzer was applied as depicted in Figure A3. This system is regarded as one of the most crucial resources used to examine the specifications of photovoltaic panels in order to display curves for the photovoltaic module, read the maximum solar energy, compute the maximum voltage, and maximum current. Test results can be saved and downloaded onto computers for subsequent examination using solar module analyzer software and an instrument interface USB optical cable.

Fig. A3. PV analyzer.

Data Logging Equipment: As seen in Figure A4, a data logger is a device that detects temperatures and has numerous channels. The surface temperature of the photovoltaic panel, the entrance water temperature to the channel, and the outflow water temperature from the channel are all vitally critical to measure after the cooling process. Anpat (AT4532) is a particular type of data logger that was chosen, and it has (32) channels. Type K and Type T thermocouples can be used with this instrument, and the read accuracy is 0.2% 1 °C.

Fig. A4. Data logger and k-type thermocouple.

Wind speed measurement: The air that passes on the device, especially when it passes on the glass cover of the solar still has a good effect on the condensation process. Therefore, the wind speed is measured by the Anemometer (AM-4206 M). The range of velocity (0.5–35.0 m/s), and power supply 9V, the accuracy of the device is from ± (2 % + 0.2 m/s). As shown in Figure A5.

Fig. A5. Wind speed measurement.

Procedures. In this work, a new idea of using a solar distillation apparatus is presented. Introduces a new mechanism for using wick materials with photocell, and using wick and Peltier indoors with PV. The wind velocity is neglected because it isn't affected on the work. The solar radiation is fixed on the 637 W/m^2.

(1) All parts of the new design have been connected and assembled.
(2) The inclination angle of the photovoltaic cell 54°.
(3) The surface of the panels should be cleaned carefully.
(4) It is necessary to fill a plastic tank with a volume of 8–10 L.
(5) The graduated cylinder was used in water flow with three different types (1, 2, 4) ml/min. The highest productivity was achieved using the wick and three Peltier as the water flow was 4 ml/min.
(6) Open the balloon, empty it of water, then put it back in.
(7) The weighing device must be zero before all-time readings are taken. The experiment started until the end of the experiment
(8) The highest productivity was determined through experiments on different types of freshwater runoff.
(9) You must wait a few minutes until the temperature of the photovoltaic module of the device reaches a stable temperature.
(10) All these experiments were conducted on different days while inside the room in the winter.
(11) Thermocouples were used in different places of the design, and their number was 24 and PV analyzer and Data Logging Equipment we will mention at once.

Appendix B

Dimensions and materials properties used in proposed modeless

Table B-1. Dimensions and materials of the unit.

Part	Materials	Items	Values (m)
PV front glass cover	Glass	Thickness	0.0032
		Length	0.539
		Width	0.66
EV layer	EV	Thickness	0.0004
		Length	0.539
		Width	0.66
PV solar cells	Silicon	Thickness	0.0003
		Length	0.539
		Width	0.66
PV back sheet	Tedler	Thickness	0.0005
		Length	0.539
		Width	0.66
Wick	Cotton	Thickness	2.1E-4
		Length	0.539
		Width	0.66
Back glass cover	Commercial glass	Thickness	0.004
		Length	0.539
		Width	0.66
Aluminum screen	Aluminum	Thickness	0.002
		Length	0.539
		Width	0.66

Table B-2. Materials properties used for PV panel.

Properties Solar cells	Description	Front glass cover	Back sheet
Density (kg/m^3)	2450	2330	1200
Thermal conductivity (K) (W/m. K)	2	130	0.15
Specific heat capacity (C) (J/kg. K)	500	677	1250
Emissivity (ϵ)	0.93	–	–
Transmissivity (Ƭ)	0.9	–	–
Backing factor	–	0.9	–
Absorptivity(α)	0.04	0.95	0.8

Table B-3. Properties of Peltier.

Properties	Specifications
Hot Side Temperature (C^O)	80
Max. Operating temperature (C^O)	138
Weight (g)	17
Q_{max} (Watts)	40
Delta T_{max} (C^O)	68
I_{max} (Amps)	6.4
V_{max} (Volts)	14.4
Module Resistance (Ohms)	0.85
Size (mm)	40–40–3.8
P–N Junction	127 couples
Material	Al2O3 (aluminum oxide)
Color	White

Table B-4. Properties of cover glass.

Properties	Value and units
Density (ρ)	2210 kg/m^3
Specific heat capacity (Cp)	730 J/kg k
Thermal conductivity(k)	1.4 w/m. k
Emissivity, Porosity (ϵ)	0.85
Thickness (t)	4 mm

Table B-5. Properties of wick cotton.

Properties	Value and units
Density (ρ)	1.52 g/cm3
Specific heat capacity (Cp)	1300 J/kg k
Thermal conductivity(k)	0.4 w/m. k
Emissivity, Porosity (ϵ)	0.72
fabric permeability (K)	0.3691 mm^2

Table B-6. Properties of aluminum screen.

Properties	Value and units
Density (ρ)	2700 kg/m^3
Specific heat capacity (Cp)	900 J/kg k
Thermal conductivity(k)	238 w/m. k
Emissivity, Porosity (ϵ)	0.62
fabric permeability (K)	^{2}

Appendix C

Calibration of solar intensity sensor

In this work, the intensity of direct solar radiation was measure by using Pyrometer device. Easy to handle in all conditions, generally acceptable accuracy and can be calibrated by comparing it to the appropriate equipment in the same measurement conditions, are the main advantages of this device. The equipment of calibration should be identical to the correct standards measurement.

Solar power meter calibration. The solar radiation measurement device (TENMARS TM-207) used in all experimental tests was calibrated with the standard Davis weather station built at Najaf Engineering Technical College/Iraq at 10 m above ground level. With a range from 0 to 1800 W/m^2 and an accuracy of ±0.3%, this station measures solar radiation in (W/m^2). The results of calibration appear in following chart (C1).

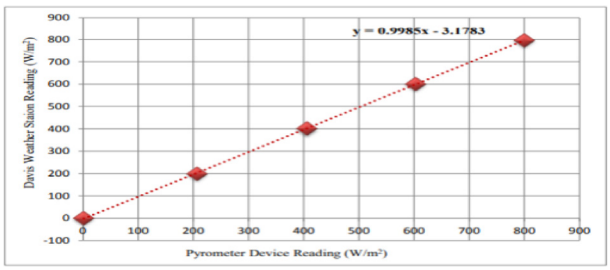

Fig. C1. Solar power meter calibration.

Wind speed sensor calibration. The type of anemometer system (AM-4206 M), with a range (0.4–30 m/s) and an accuracy (±1.8% N+2d) was used to measure wind speed in this work. This device is simple to manage under all conditions and can be adjusted by comparing it to the required equipment under the same measurement conditions, with generally acceptable precision. The calibration equipment must be similar to the proper level of measurement.

The type of wind speed measurement device (anemometer) (AM-4206 M) used in all experimental tests has been calibrated with the standard Davis weather station built at Najaf Engineering Technical College/Iraq at 10 m above ground level. The wind speed of this station is measured in (m/s) with a range of 0.1–89 m/s and ±5 % accuracy. The results of the calibration appear in the following chart (C2).

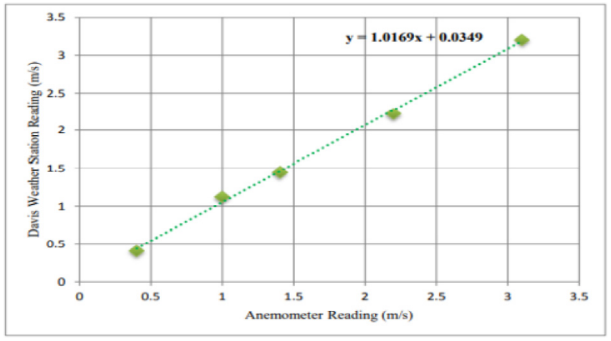

Fig. C2. Anemometer calibration.

References

1. Kabeel AE, El-Agouz SA. Review of researches and developments on solar stills. *Desalination*. 2011;276:1–12.
2. Kabeel AE, Arunkumar T, Denkenberger DC, Sathyamurthy R. Performance enhancement of solar still through efficient heat exchange mechanism – a review. *Appl Therm Eng*. 2017;114:815–836.
3. Sathyamurthy R, El-Agouz SA, Nagarajan PK, Subramani J, Arunkumar T, Mageshbabu D, et al. A Review of integrating solar collectors to solar still. *Rev Integr Sol Collect Sol*. 2017;77:1069–1097. ISSN 1364-0321, https://doi.org/10.1016/j.rser.2016.11.223.
4. Kumar S, Tiwari GN. Estimation of internal heat transfer coefficients of a hybrid (PV/T) active solar still. *Sol Energy*. 2009;83:1656–1667.
5. Dev R, Centre GNT. Characteristic equation of a hybrid (PV-T) active solar still. *Desalination J*. 2010;51:126–137.
6. Kumar S, Tiwari A. Design, fabrication and performance of a hybrid photovoltaic/thermal (PV/T) active solar still. *Energy Convers Manag J*. 2010;51:1219–1229.
7. Gaur MK, Tiwari GN. Optimization of number of collectors for integrated PV/T hybrid active solar still. *Appl Energy*. 2010;87:1763–1772.
8. Eltawil MA, Omara ZM. Enhancing the solar still performance using solar photovoltaic, flat plate collector and hot air. *Desalination*. 2014;349:1–9.
9. Saeedi F, Sarhaddi F, Behzadmehr A. Optimization of a PV/T (photovoltaic/thermal) active solar still. *Energy*. 2015;87:142–152.
10. Al-Nimr MA, Al-Ammari WA. A novel hybrid PV-distillation system. *Sol Energy*. 2016;135:874–883.

11. Tiwari GN, Yadav JK, Singh DB, Al-Helal IM, Dbdel-Ghany AM. Exergoeconomic and enviroeconomic analyses of partially covered photovoltaic flat plate collector active solar distillation system. *Desalination J*. 2015;367:186−196.
12. Yari M, Mazareh AE, Mehr AS. A novel cogeneration system for sustainable water and power production by integration of a solar still and PV module. *Desalination*. 2016;398:1−11.
13. Riahia A, Yusof KW, Singh BSM, Isa MH, Olisa E, Zahari NAM. Sustainable potable water production using a solar still with photovoltaic modules-AC heater. *Desalination Water Treat*. 2015;57:32.
14. Pansal K, Ramani B, Sadasivuni KK, Panchal H, Manokar M, Sathyamurthy R, et al. Use of solar photovoltaic with active solar still to improve distillate output: a review. *J Pre-Proof Use*. 2020;10:1−8, 100341, ISSN 2352-801X, https://doi.org/10.1016/j.gsd.2020.100341.
15. Abed AF, Hachim DM, Najim SE. A novel hybrid PV/T system for sustainable production of distillate water from the cooling of the PV module. *IOP Conf Ser Mater Sci Eng*. 2021;1094:012049.
16. Najafi H, Woodbury KA. Optimization of a cooling system based on Peltier effect for photovoltaic cells. *Sol Energy*. 2013;91:152−160.